Protection and Control of Modern Power Systems

ORIGINAL RESEARCH Open Access

Comprehensive power swing detection by current signal modeling and prediction using the GMDH method

Seyed Amir Hosseini[1], Behrooz Taheri[2], Hossein Askarian Abyaneh[3*] and Farzad Razavi[2]

Abstract

Power swing is an undesirable variation in power flow. This can be caused by large disturbances in demand load, switching, disconnection or reclosing lines. This phenomenon may enter the zones of distance relays and cause relay malfunction leading to the disconnection of healthy lines and undermining network reliability. Accordingly, this paper presents a new power swing detection method based on the prediction of current signal with a GMDH (Group Method of Data Handling) artificial neural network. The main advantage of the proposed method over its counterparts is the immunity to noise effect in signals. In addition, the proposed method can detect stable, unstable, and multi-mode power swings and is capable of distinguishing them from the variety of permanent faults occurring simultaneously. The method is tested for different types of power swings and simultaneous faults using DIgSILENT and MATLAB, and compared with some latest power swing detection methods. The results demonstrate the superiority of the proposed method in terms of response time, the ability to detect power swings of different varieties, and the ability to detect different faults that may occur simultaneously with power swings.

Keywords: Power swing, Distance relay, Power system protection, GMDH

1 Introduction

Distance relays are widely used in power systems to protect transmission lines [1, 2]. Despite their excellent features and contributions to power system protection, these relays may malfunction during power swings, leading to the tripping of healthy lines. Such malfunction could lead to power system instability and cause a major power outage. To prevent this, distance relays are equipped with a power swing blocking (PSB) function. The mechanisms of power swing detection and PSB activation in distance relays have been the subject of many studies.

In [3, 4], several detection methods based on the rate of impedance change are proposed. These can distinguish between slow power swings and faults, and block the distance relay when necessary. However, they cannot detect fast power swings nor faults that occur simultaneously with power swings [5–9]. Reference [5] proposes a power swing/fault differentiation method based on the observed resistance in the distance relay. This method functions on the idea that the resistance observed in the relay during a power swing is constantly changing whereas it remains largely constant during a fault. However, this method requires a long time to detect power swings. In [7], a power swing detection method based on a combination of a concentric impedance characteristic and continuous monitoring of apparent impedance is proposed, whereas in [10], power swings are detected based on the swing center voltage (SCV). In [11], power swings are detected using the Fast Fourier Transform (FFT) of the DC component of the current, though one of the problems of FFT-based techniques is on setting suitable threshold values for

* Correspondence: askarian@aut.ac.ir
[3]Department of Electrical Engineering, Amirkabir University of Technology, Tehran, Iran
Full list of author information is available at the end of the article

fault detection [12]. In addition, such techniques use asynchronous sampling with a limited number of samples. This makes them vulnerable to problems such as spectral leakage and the picket fence effect [13, 14]. In [15], wavelet transform is used to avoid the FFT problems. In this method power swings and simultaneous faults are detected based on the harmonics derived from a wavelet transform. Reference [16] uses a fast wavelet transform algorithm to detect symmetrical faults that occur simultaneously with a power swing, while in [17], power swings and faults are detected by applying the wavelet transform to impedance changes. In [18], wavelet transform analysis of current changes is used to detect faults with different resistances during power swings.

Reference [19] proposes a power swing detection method based on the window averaging of current. However, such a method may malfunction under multi-mode power swings, and it is unable to detect asymmetrical power swings. In [20], power swings are detected based on the rate of changes in the RMS values of current during faults and power swings. Although this method is capable of detecting high impedance faults during power swings, it cannot detect asymmetrical one-phase power swings induced by single-pole switching. In [21], faults are differentiated from power swings by analyzing the rate of instantaneous frequency changes. However, this method is noise sensitive and is unable to detect multi-mode power swings. A detection method based on the rate of changes in the average apparent power is proposed in [22]. This can properly detect multi-mode power swings but not the asymmetrical ones. A method based on zero-frequency filtering is presented in [23] and can detect fast three-phase faults that occur at the same time as a power swing [24]. However, it cannot properly detect multi-mode power swings and could malfunction when the signals are noisy. The detection method provided in [25] uses a fast wavelet transform, which can detect three-phase faults during power swings but requires a high sampling rate (20 kHz) and changes in sampling rate at different times. In [26], a detection method based on the rate of change in the kinetic energy signal is proposed. This method can detect various types of faults during power swings but underperforms during multi-mode power swings. Reference [27] proposes a new method based on the Fourier transform. It provides fast calculation and fault detection along with power swings. However, it lacks the capability to detect unbalanced power swings. In [28], a method based on the theory of signal compression is proposed which requires a lower sampling rate. However, although lower sampling rate leads to high-speed fault detection, it also increases the likelihood of misdiagnosis. A fault detection method with power swing based on mathematical morphology is proposed in [29]. However, the method may make a false disconnection of healthy lines during a multi-mode power swing. A method based on the prediction of signal samples using phaselet transform is proposed in [30], though it needs a longer time for detecting faults that occur during a power swing and determining the appropriate threshold value is also very challenging. A method based on empirical mode decomposition is proposed in [31], which has the outstanding feature of being capable to detect a multi-mode power swing. However, the main limitation on its application is the strong dependence on the correct determination of the number of intrinsic mode functions (IMFs), as the presented method can lead to erroneous IMFs in networks with different topologies.

In summary, the methods in the literature all have shortcomings which limit their use. To address the problems, this paper presents a new power swing detection method based on the prediction of current signals by the Group Method of Data Handling (GMDH). The main advantage of the proposed method over its counterparts is its immunity to noise. In addition, the method can detect all types of stable, unstable, and multi-mode power swings and can properly distinguish all types of permanent faults that occur simultaneously with these power swings. Also, the performance of this method is independent of the network structure. The proposed method is tested on the standard IEEE 39-bus network and a standard 9-bus network for different power swings and simultaneous faults. The results demonstrate the success of the method in detecting all types of power swings and simultaneous faults. Moreover, a comparison of the results with those of existing relay protection methods shows its superiority in terms of response speed and the diversity of power swings covered.

The rest of this paper is structured as follows. The proposed method is presented in Section 2, which describes the GMDH neural network and explains how signals are predicted. Section 3 presents the results of the tests performed on the standard IEEE 39-bus network and a standard 9-bus network under different power swings and simultaneous faults. In Section 5, the proposed method is compared with the existing alternatives, and Section 6 draws the conclusions.

2 Power swing

Figure 1 is presented to better understand or illustrate the concept of power swing and instability in a power system. The electric power (P_e) and its maximum value (P_{Max}) can be obtained in pu as [32, 33]:

$$P_e = \frac{E_1.E_2}{X_T}\ \sin\delta \tag{1}$$

$$P_{Max} = \frac{E_1.E_2}{X_T} \tag{2}$$

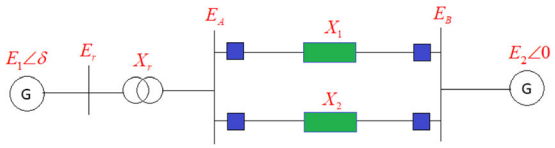

Fig. 1 Single-line diagram of a typical double fed network

where X_T is the total network impedance and δ is the rotor angle (in electric radians).

According to Fig. 1, if both transmission lines between buses A and B are active, the changes in $P-\delta$ are shown in Fig. 2. In this state, for a given input mechanical power P_m, the output steady-state electrical power P_e will be equal to P_m and the operating point is at "a" as shown in Fig. 2. If one of the lines is disconnected, the effective reactance X_T will increase and the changes in $P-\delta$ are also shown in Fig. 2. As illustrated, in this state, the maximum power is reduced, while the rotor angle will rise to transfer the same steady-state power so the rotor angle δ_0 corresponds to the working point "b" in Fig. 2. The swing equation is expressed as [32]:

$$\frac{2H}{\omega_0}\frac{d^2\delta}{dt^2} = P_m - P_{Max}\sin\delta \tag{3}$$

where P_m is the input of mechanical power (in pu), H is the inertial constant (in MWS/MVA), and t is time (in seconds).

3 Proposed method

3.1 GMDH neural network

With the rapid progress of artificial neural networks in recent decades, they have become a viable alternative to traditional computing methods. Artificial neural networks take a series of observations as the inputs of a training phase. This enables them to predict similar time series in the future. The GMDH neural network is a polynomial neural network that was first introduced by Grigorevich in 1968.

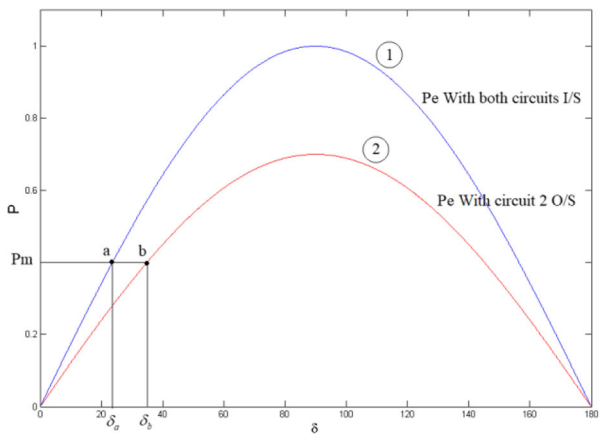

Fig. 2 Changes in $P-\delta$ for the network in Fig. 1

The reason for working with the GMDH model is its superiority over conventional neural networks. In [34], it is confirmed that the GMDH neural network performs much better than conventional neural networks (e.g., MLP and LSM Tree) in time series modeling. In addition, GMDH needs much less training time than Deep Learning methods and models such as LSTM, and does not require complex hardware for training. The basic GMDH model is shown in Fig. 3, and can be expressed in the form of:

$$y = a_0 + \sum_{i=1}^{n} a_i f_i \tag{4}$$

where y is the system output, a_0 is a constant, a_i denotes the weight coefficients, f_i denotes the basic functions, and n is the total number of inputs. The basic model of (4) can be rewritten based on the Kolmogorov-Gabor polynomial as:

$$y = a_0 + \sum_{i=1}^{n} a_i x_i + \sum_{i=1}^{n}\sum_{j=1}^{n} a_{ij} x_i x_j + \ldots \tag{5}$$

where x is the system input. The number of terms in (5) strongly depends on the number of inputs and can be calculated by:

$$\text{Number of sentences} = 2^n \tag{6}$$

According to (6), the number of terms in (5) rapidly increases with the complexity of the system. For example, the number of terms for 30 inputs reaches 10^{10} as:

$$2^{30} \simeq \left(2^3\right)^{10} \simeq 10^{10} \tag{7}$$

For such a large number, it would be very difficult to find its coefficients. The issue can be resolved by using the method presented in Fig. 4, which uses a group of efficient models to reach a general model. This approach involves decomposing the problem of (5) into several problems with fewer unknown variables and then solving each of these smaller problems as parts of a larger problem. In this approach, partial models are obtained using the least-squares method.

Assuming that there are four inputs x_1, x_2, x_3, and x_4, the general model is given as:

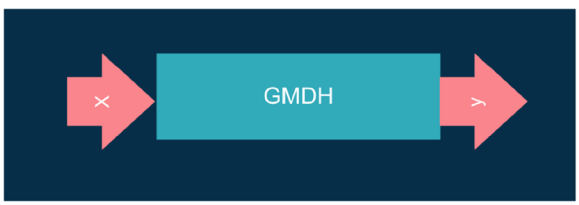

Fig. 3 Basic GMDH model

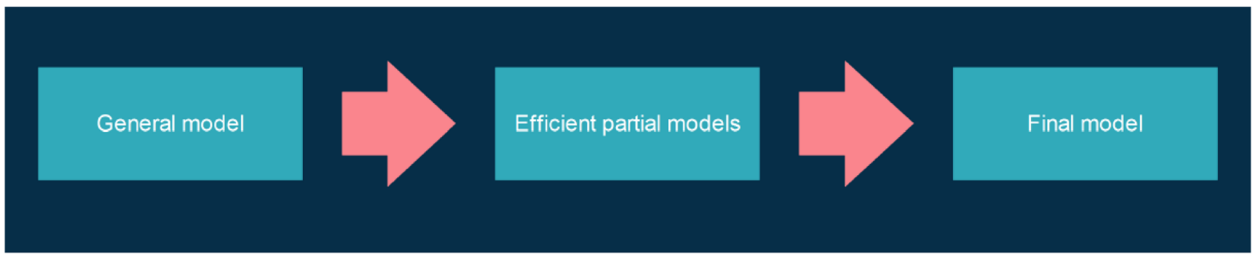

Fig. 4 Mechanism of using efficient models to reach a general model

$$y = a_0 + \sum_{i=1}^{n} a_i x_i + \sum_{i=1}^{n}\sum_{j=1}^{n} a_{ij} x_i x_j + \sum_{i}^{n}\sum_{j}^{n}\sum_{k}^{n} a_{ijk} x_i x_j x_k + \sum_{i}^{n}\sum_{j}^{n}\sum_{k}^{n}\sum_{l}^{n} a_{ijkl} x_i x_j x_k x_l \quad (8)$$

Equation (8) can be turned into multiple problems with fewer unknowns using the following:

$$Z_{ij} = c_1 + c_2 x_i + c_3 x_j + c_4 {x_i}^2 + c_5 {x_j}^2 + c_6 x_i x_j \quad (9)$$

In (9), Z_{ij} is the temporary output and c_1- c_6 are the coefficients of the terms, which can be calculated by (10)–(19) shown below.

Figure 5 shows a simple artificial neural network model. In this simplified network, Z is computed based on x_i and x_j using (9). To implement the procedure of Fig. 5, all samples obtained from (9) should be turned into a vector similar to the following:

$$y \simeq Z = \begin{bmatrix} c_1 & c_2 & c_3 & c_4 & c_5 & c_6 \end{bmatrix} \begin{bmatrix} 1 \\ x_i \\ x_j \\ x_i^2 \\ x_j^2 \\ x_i x_j \end{bmatrix} \quad (10)$$

Equation (10) can be rewritten as:

$$y = c^T x_{ij} \quad (11)$$

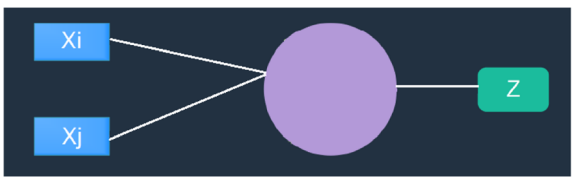

Fig. 5 A simple artificial neural network model

If all existing samples are considered in (11), then there are:

$$\begin{cases} y_1 = c^T x_1 \\ y_2 = c^T x_2 \\ . \\ . \\ . \\ y_n = c^T x_n \end{cases} \quad (12)$$

$$\underbrace{\begin{bmatrix} y_1 & y_2 & \dots & y_n \end{bmatrix}}_{Y} = c^T \underbrace{\begin{bmatrix} x_1 & x_2 & \dots & x_n \end{bmatrix}}_{X} \quad (13)$$

Using (12) and (13), the general equation is formulated as:

$$Y = c^T X \quad (14)$$

To obtain the c^T values, both sides of (14) are multiplied by X^T, i.e.:

$$YX^T = c^T XX^T \quad (15)$$

Multiplying by $(XX^T)^{-1}$ on both sides of (15) yields:

$$YX^T\left(XX^T\right)^{-1} = c^T \underbrace{\left(XX^T\right)\left(XX^T\right)^{-1}}_{1} \quad (16)$$

$$c^T = YX^T\left(XX^T\right)^{-1} \quad (17)$$

c^Tcan be calculated by having the right pseudoinverse of matrix X as:

$$X^{\dagger} = X^T\left(XX^T\right)^{-1} \quad (18)$$

$$c^T = YX^{\dagger} \quad (19)$$

According to (10)–(19) and Fig. 6, the above procedure turns the four initial inputs into six, thus making the system more complex. To avoid this issue, a measure is proposed for choosing $Z_{ij's}$ based on the type of problem.

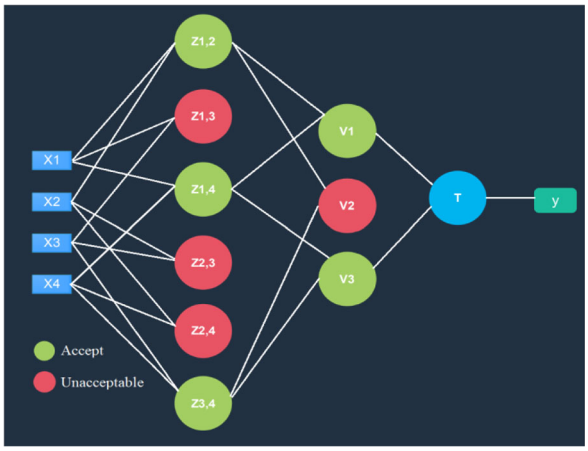

Fig. 6 GMDH neural network model

Using the proposed measure, a number of $Z_{ij's}$ will be selected and the rest will be discarded. Then, the selected $Z_{ij's}$ will be used to another layer and the previous steps will be repeated. The stopping condition is to reach one neuron.

3.2 Training of GMDH neural network

To function correctly, neural networks have to be trained with a wide variety of fault and power swing data. In this study, the GMDH neural network model is trained for the double-fed network shown in Fig. 7.

The training is performed using the data obtained from 16 simulations, the details of which are given in Table 1. In these simulations, the distance relay is placed to protect Line A. After applying various types of power swings to Line A, the outcomes are recorded for use in training. In this study, power swings are detected based on the difference between the predicted value and the real value of the signal. Therefore, these simulations are performed without injecting any faults in order to increase the difference between the predicted and real signals during the occurrence of a fault.

Figure 8 shows the training of the neural network model, which consists of three sections, i.e., one for training data, one for test data, and the other for all data.

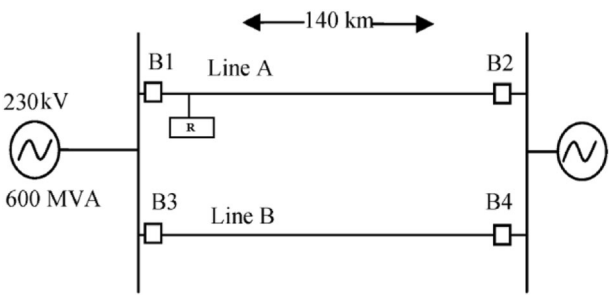

Fig. 7 Double-fed 230 kV network

Table 1 Details of simulations performed on the network in Fig. 7 to train the neural network model

Case study	Power swing frequency (Hz)
1	1
2	1
3	1
4	2
5	2
6	2
7	3
8	3
9	3
10	4
11	4
12	4
13	5
14	5
15	5
16	Unstable power swing
17	Multi-mode power swing

In all three sections, the x-axis is the target output and the y-axis is the output of the neural network. The neural network functions correctly when the curve falls on the Y = T line (the line with a y-intercept of zero and slope of 1). As shown in Fig. 8, the neural network performs very well for both training and test data and ultimately achieves a regression coefficient of 1 in all cases.

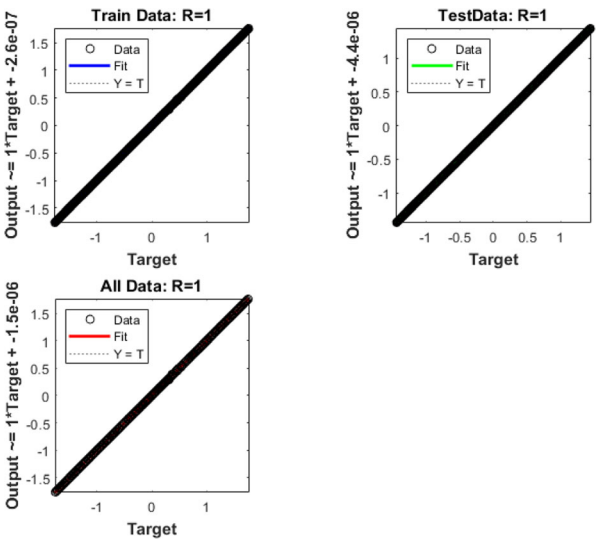

Fig. 8 Training of the neural network model

3.3 Signal prediction

The parameters that need to be predicted during a power swing and after a fault can be expressed as [30]:

$$f(t) = A\ \cos(2\pi f_2 t) \cdot\ \cos(2\pi f_1 t + \theta) \tag{20}$$

$$f(t) = Be^{f_s t \cdot e^{\frac{-1}{\tau f_s}}} \cdot\ \cos(2\pi f_1 t + \theta) \tag{21}$$

From the above equations, it can be deduced that current samples can be predicted more successfully under normal and power swing conditions than after a fault, because of the presence of a damping component during a fault. Under normal conditions, there is no DC component in the current waveform. It is thus necessary to eliminate the DC component from the real samples before comparing them with predicted values. The input current and the real samples can be expressed as:

$$i(t) = I_m\ \sin(\omega t + \theta) \tag{22}$$

$$sample^*(n+1)_{actual} = sample(n+1)_{actual} - \sum_{g=0}^{N-1} sample(n-g+1)_{actual} \tag{23}$$

Thus, the difference between the predicted and real signal values can be calculated by:

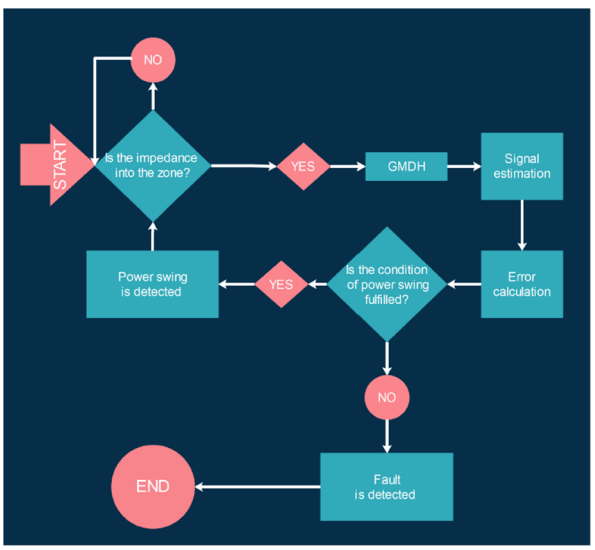

Fig. 9 Algorithm of the proposed method

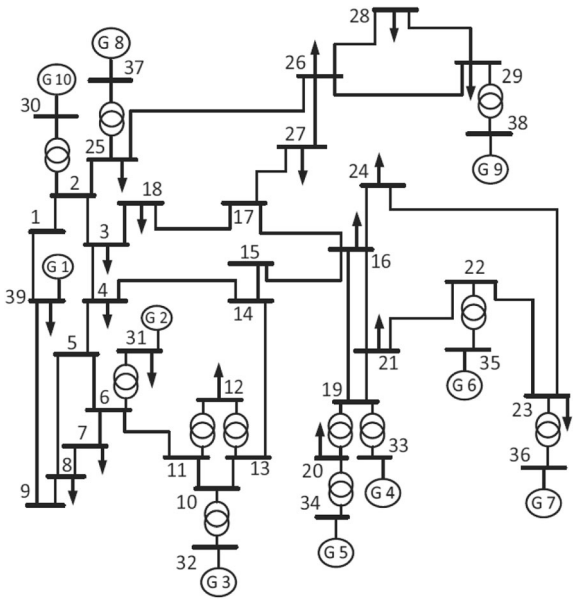

Fig. 10 Single-line diagram of the standard IEEE 39-bus network

$$Error(n+1) = abs(sample(n+1)_{estimated} - sample^*(n+1)_{actual}) \tag{24}$$

Therefore, the effective difference between the predicted and real signal values is given as:

$$RMSE = \sqrt{\frac{\sum_{k=1}^{N} Error^2}{N}} \tag{25}$$

The outputs of (25) determine the state of the power network. If the RMSE is larger than the threshold value, a fault has occurred. In contrast, if the RMSE is smaller than the threshold value, the network is either in a normal condition or is experiencing a power swing. If the RMSE is lower than the threshold value and the

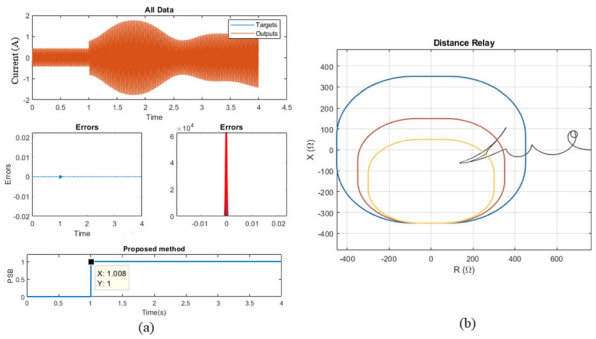

Fig. 11 **a** Performance of the proposed algorithm under the applied stable power swing. **b** Impedance changes during the applied stable power swing

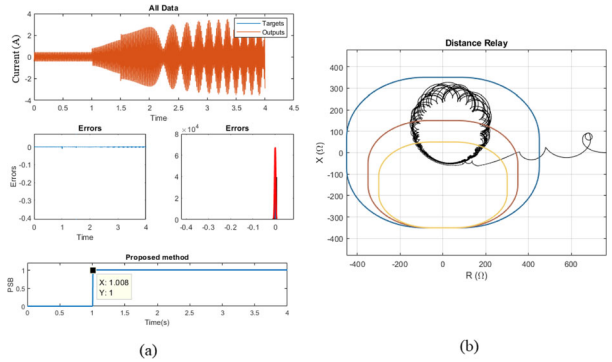

Fig. 12 a Performance of the proposed algorithm under the applied unstable power swing. **b** Impedance changes during the applied unstable power swing

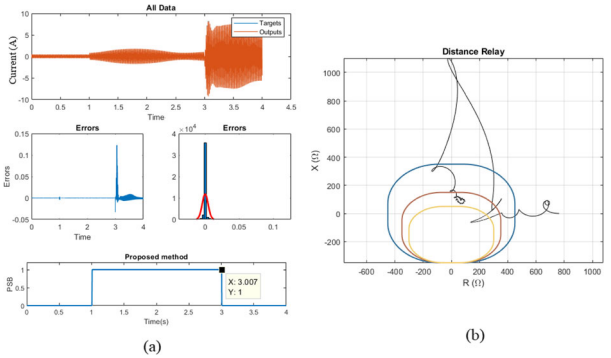

Fig. 14 a Performance of the proposed algorithm under the single-phase fault occurring simultaneously with power swings. **b** Impedance changes during the single-phase fault occurring simultaneously with power swings

impedance observed by the distance function falls within the protection zone, there is a power swing in the system. The algorithm of the proposed method is illustrated in Fig. 9.

4 Simulation results

4.1 Test on the IEEE 39-bus network

The proposed method is tested and evaluated using the standard IEEE 39-bus network in the DIgSILENT software. The single-line diagram of this network is shown in Fig. 10. This network consists of 39 buses, 10 generators, and 19 load points, which consume 6150.1 MW of active power and 1233.9 MVar of reactive power. The distance relay chosen for implementing the proposed method is placed on Bus 26 to protect Lines 26–29. Using DIgSILENT, a variety of power swings and faults are applied to the network.

4.1.1 Stable power swing

A power swing occurs when the rotor angle of a generator advances or retards relative to others. This phenomenon may occur because of changes in load size and direction, line switching, loss of generator excitation, or faults. In the cases where the generator with the mismatching rotor angle does not experience pole slip and the system reaches a new equilibrium, it is said that a stable swing power has occurred. To simulate a stable power swing on Line 26–29, the breakers on the parallel Lines 26–28 and 28–29 are opened at t = 1 s. The performance of the proposed algorithm under this power swing is shown in Fig. 11a, while Fig. 11b displays the impedance changes during the power swing.

4.1.2 Unstable power swing

Unstable power swings occur when the events described in the previous section lead to the occurrence of pole slip in one or more generators. To simulate the strongest type of unstable power swing, the breakers at the parallel Lines 26–28 and 28–29 are opened at t = 1 s, and a large load of 2000 MW and 200 MVar is then applied to Bus 26 at t = 1.5 s. The performance of the proposed algorithm under this unstable power swing is illustrated in

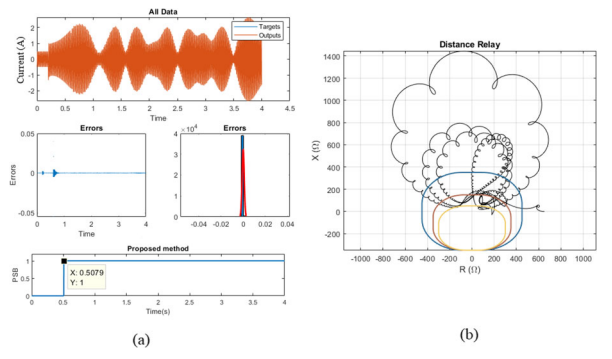

Fig. 13 a Performance of the proposed algorithm under the applied multi-mode power swing. **b** Impedance changes during the applied multi-mode power swing

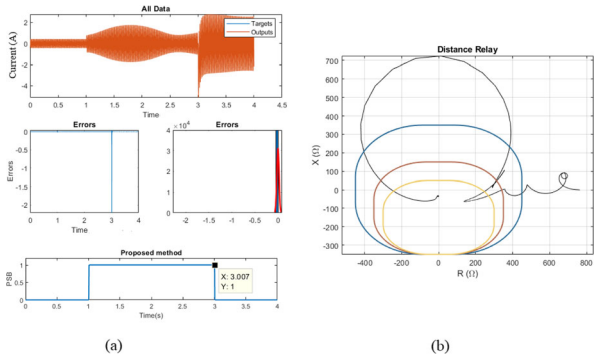

Fig. 15 a Performance of the proposed algorithm under the three-phase fault occurring simultaneously with power swings. **b** Impedance changes during the three-phase fault occurring simultaneously with power swings

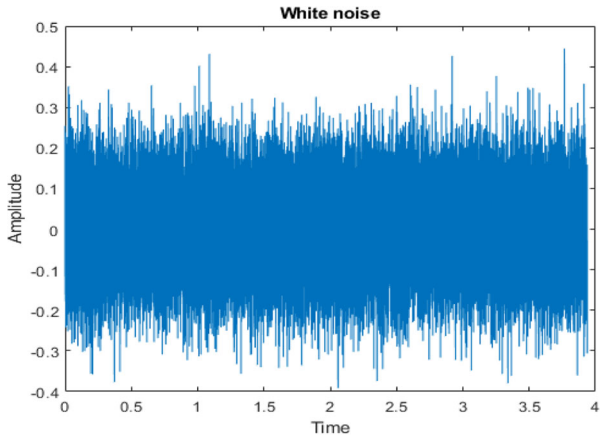

Fig. 16 White Gaussian noise added to the unstable power swing

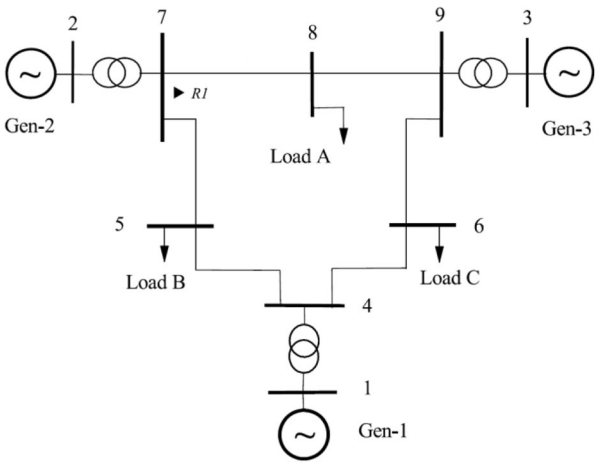

Fig. 18 Single-line diagram of the standard 9-bus network

Fig. 12a, while Fig. 12b shows the impedance changes. As seen, the proposed algorithm is successful in detecting this unstable power swing and blocking the relay in time.

4.1.3 Multi-mode power swing

Multi-mode power swings occur when a power swing involves two or more machines and therefore current and voltage phasors are not completely sinusoidal [35]. To simulate a multi-mode power swing, a three-phase fault is applied to Line 4–14. This fault starts at t = 0.2 s and the line is tripped by the breaker at t = 0.6 s. The performance of the algorithm under this power swing is illustrated in Fig. 13a and the impedance changes during this multi-mode power swing are plotted in Fig. 13b. As shown in Fig. 13a, the proposed algorithm detects the multi-mode power swing and activates the PSB function accordingly.

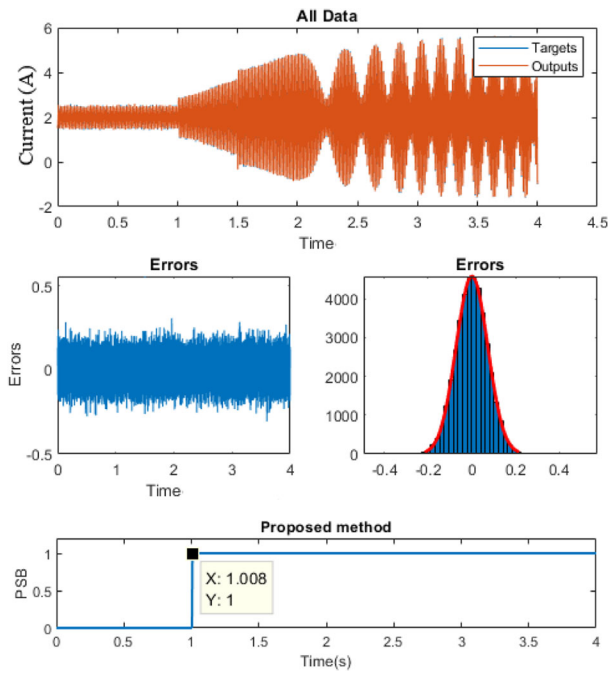

Fig. 17 Performance of the proposed method under noisy signal

4.1.4 Single-phase fault occurring simultaneously with power swings

To evaluate the response of the proposed algorithm to single-phase faults, a single-phase line-to-ground fault is applied to Line 26–29. To create the power swing, the line parallel to Line 26–29 is tripped at t = 1 s, while at t = 3 s, a single-phase fault is applied to the same line. The performance of the proposed algorithm under this fault is illustrated in Fig. 14a while Fig. 14b shows the impedance changes. As shown in Fig. 14a, during the

Table 2 Performance of the proposed method under different faults in the standard two-area network

Power swing type	Fault inception (sec)	Fault location in line 8–9 (%)	Proposed method fault detection (ms)
Stable power swing	5	10	7
	5	90	8
	5.01	10	7
	5.01	90	7
	5.016	10	7
	5.016	90	8
Unstable power swing	5	10	7
	5	90	7
	5.01	10	7
	5.01	90	8
	5.016	10	7
	5.016	90	7

Table 3 Comparison with alternative methods

Ref. No	Method	Unstable power swing	three-phase fault with a phase angle of 180 degrees	Multi-mode power swing	Noise
[19]	Moving window averaging	Yes	Yes	No	No
[21]	Instantaneous frequency	Yes	Yes	No	No
[22]	Apparent Power	Yes	No	No	No
[36]	Rate of change of power	Yes	No	No	No
Proposed method	**GMDH**	**Yes**	**Yes**	**Yes**	**Yes**

power swing, the relay function is correctly blocked. After the occurrence of the fault, it is detected in 7 milliseconds and the PSB function is properly disabled.

4.1.5 Three-phase fault occurring simultaneously with power swings

Because of the symmetrical nature of power swings, most existing power swing detection algorithms cannot properly distinguish between power swings and three-phase faults. In contrast, the proposed method is capable of detecting three-phase faults with high precision, an ability attributable to the conditions included in its mechanism and the use of the initial transient state of faults in the design. Given the defined conditions, when a fault occurs, the rate of change rises above the threshold value and the relay is thus unblocked. In the study, this fault is simulated by applying a three-phase fault to Line 26–29 at t = 3 s, while the performance of the method is shown in Fig. 15a with Fig. 15b illustrating the impedance changes. As can be seen from Fig. 15a, upon the occurrence of a power swing, the PSB function successfully blocks the relay, but once the three-phase fault occurs, the algorithm detects the fault and unblocks the relay.

4.1.6 Effect of noise on the performance of the proposed method

Signals can be affected by white noise, which can severely undermine the accuracy of power swing detection algorithms [27, 28]. To evaluate the performance of the proposed algorithm in the presence of noise, it is tested under an unstable power swing with white Gaussian noise. In the study, a white Gaussian noise signal which has a signal-to-noise ratio of 30 dB and a variance of 0.05, as shown in Fig. 16, is added to the unstable power swing current signal.

As shown in Fig. 17, the proposed algorithm correctly detects the unstable power swing with white Gaussian noise and blocks the relay.

4.2 Test on the standard 9-bus network

The effect of different types of faults on the performance of the proposed method is studied on a standard 9-bus network. The single-line diagram of this network is displayed in Fig. 18, and more detailed information about this network can be found in [23].

The results obtained using this standard 9-bus network are provided in Table 2. They demonstrate the ability of the method to detect all types of fast and slow power swings and the variety of faults that may occur simultaneously. For better evaluation of the proposed method, its responses to different faults applied at different times and positions are investigated. As shown in Table 2, the proposed method has a very high response speed and exhibits an adequate performance for all types of faults.

5 Comparison with the existing alternatives for protection relays

In Table 3, the proposed method and other existing power swing detection methods are compared in terms of performance under high impedance faults, multi-mode power swings, a three-phase fault with a phase angle of 180 degrees, and noisy signals. It shows that while other methods experience difficulty in dealing with high impedance faults and noisy signals, the proposed method performs very well in this area.

6 Conclusion

This paper has presented a high-performance highly reliable method for the detection of power swings and faults that may occur simultaneously. In the proposed method, a signal prediction mechanism based on GMDH is used to distinguish between power swings and faults. The proposed method is tested for power swings of the stable, unstable, and multi-mode variety and various types of single-phase and three-phase faults on a test network. The results demonstrate the ability of the proposed method to respond correctly and swiftly to different types of power swings and simultaneous faults. Compared to the methods commonly used in protective relays which have difficulties in detecting some types of power swings, the proposed method can detect all types of power swings.

Abbreviations

GMDH: Group Method of Data Handling; PSB: Power Swing Blocking; SCV: Swing Center Voltage; FFT: Fast Fourier Transform; IMF: Intrinsic Mode Function; MLP: Multi-Layer Perceptron; LSM: Liquid State Machine; LSTM: Long Short-Term Memory

Acknowledgements

Not applicable.

Authors' contributions
The paper was a collaborative effort among the authors. SAH and BT, brings up the idea by GMDH for power swing blocking, performed the primary simulations and drafted the manuscript. HAA and FR, participated in enriching the manuscript (in theoretical idea and simulation section (IEEE 9-Bus power system)) and carried out the revising the manuscript (editing grammatical and lexical mistakes). All authors read and approved the final manuscript.

Funding
Not applicable.

Availability of data and materials
Please contact author for data requests.

Declarations

Competing interests
The authors declare that they have no competing interests.

Author details
[1]Department of Electrical Engineering, Golpayegan University of Technology, Isfahan, Iran. [2]Faculty of Electrical, Biomedical and Mechatronics Engineering, Qazvin Branch, Islamic Azad University, Qazvin, Iran. [3]Department of Electrical Engineering, Amirkabir University of Technology, Tehran, Iran.

Received: 18 August 2019 Accepted: 30 March 2021
Published online: 16 April 2021

References
1. Zubić, S., Balcerek, P., & Zeljković, Č. (2017). Speed and security improvements of distance protection based on discrete wavelet and Hilbert transform. *Electric Power Systems Research*, *148*, 27–34. https://doi.org/10.1016/j.epsr.2017.03.013.
2. Taheri, B., Hosseini, S. A., Askarian-Abyaneh, H., & Razavi, F. (2019). A new method for remote testing distance relay using internet protocol version 4. In *2019 international conference on protection and automation of power system (IPAPS)*, (pp. 31–37). Iran: IEEE.
3. Kundur, P., Balu, N. J., & Lauby, M. G. (1994). *Power system stability and control, vol. 7*. New York: McGraw-hill.
4. Gao, Z., & Wang, G. (1991. APSCOM-91., 1991 International Conference on 1991). A new power swing block in distance protection based on a microcomputer-principle and performance analysis. In *Advances in Power System Control, Operation and Management*, (pp. 843–847). Hong Kong: IET.
5. Khoradshadi-Zadeh, H. (2005). Evaluation and performance comparison of power swing detection algorithms. In *Power engineering society general meeting, 2005*, (pp. 1842–1848). San Francisco: IEEE.
6. Lin, X., Li, Z., Ke, S., & Gao, Y. (2010). Theoretical fundamentals and implementation of novel self-adaptive distance protection resistant to power swings. *IEEE Transactions on Power Delivery*, *25*(3), 1372–1383. https://doi.org/10.1109/TPWRD.2010.2043450.
7. Martuscello, L., Krizauskas, E., Holbach, J., & Lu, Y. (2009). Tests of distance relay performance on stable and unstable power swings reported using simulated data of the august 14 th 2003 system disturbance. In *Power systems conference, 2009. PSC'09*, (pp. 1–21). Clemson: IEEE.
8. Mahamedi, B. (2010). A very fast unblocking scheme for distance protection to detect symmetrical faults during power swings. In *IPEC, 2010 conference proceedings*, (pp. 378–383). Singapore: IEEE.
9. Nayak, P. K., Rao, J. G., Kundu, P., Pradhan, A., & Bajpai, P. (2010 Joint International Conference on 2010). A comparative assessment of power swing detection techniques. In *Power electronics, drives and energy systems (PEDES) & 2010 power India*, (pp. 1–4). New Delhi: IEEE.
10. Benmouyal, G., Hou, D., & Tziouvaras, D. (2004). Zero-setting power-swing blocking protection. In *31st Annual Western Protective Relay Conference*, (pp. 19–21).
11. Karegar, H. K., & Mohamedi, B. (2009. ECTI-CON 2009. 6th international conference on 2009). A new method for fault detection during power swing in distance protection. In *Electrical engineering/electronics, computer, telecommunications and information technology*, (pp. 230–233). Chonburi: IEEE.
12. Mahamedi, B., & Zhu, J. G. (2012). A novel approach to detect symmetrical faults occurring during power swings by using frequency components of instantaneous three-phase active power. *IEEE Transactions on Power Delivery*, *27*(3), 1368–1376. https://doi.org/10.1109/TPWRD.2012.2200265.
13. Li, Y. F., & Chen, K. F. (2008). Eliminating the picket fence effect of the fast Fourier transform. *Computer Physics Communications*, *178*(7), 486–491. https://doi.org/10.1016/j.cpc.2007.11.005.
14. Ahmad, H., Salam, M., Ying, L. Y., & Bashir, N. (2008). Harmonic components of leakage current as a diagnostic tool to study the aging of insulators. *Journal of Electrostatics*, *66*(3–4), 156–164. https://doi.org/10.1016/j.elstat.2007.11.004.
15. Brahma, S. (2006. IEEE 2006). Use of wavelets for out of step blocking function of distance relays. In *Power engineering society general meeting*, (p. 5). Montreal: IEEE.
16. Pang, C., & Kezunovic, M. (2010). Fast distance relay scheme for detecting symmetrical fault during power swing. *IEEE Transactions on Power Delivery*, *25*(4), 2205–2212. https://doi.org/10.1109/TPWRD.2010.2050341.
17. Mahamedi, B. (2011 2nd international conference on 2011). A new power swing blocking function based on wavelet transform. In *Electric power and energy conversion systems (EPECS)*, (pp. 1–6). Sharjah: IEEE.
18. Dubey, R., Samantaray, S., Tripathy, A., Babu, B. C., & Ehtesham, M. (2012 Students conference on 2012). Wavelet based energy function for symmetrical fault detection during power swing. In *Engineering and systems (SCES)*, (pp. 1–6). Allahabad: IEEE.
19. Rao, J. G., & Pradhan, A. K. (2015). Power-swing detection using moving window averaging of current signals. *IEEE Transactions on Power Delivery*, *30*(1), 368–376. https://doi.org/10.1109/TPWRD.2014.2342536.
20. Taheri, B., & Razavi, F. (2018). Power swing detection using rms current measurements. *Journal of Electrical Engineering & Technology*, *13*(5), 1831–1840.
21. Taheri, B., Salehimehr, S., Razavi, F., & Parpaei, M. (2019). Detection of power swing and fault occurring simultaneously with power swing using instantaneous frequency. *Energy Systems, 11* 1–24.
22. Taheri, B., Razavi, F., & Salehimehr, S. (2019). Power swing detection using the variation rates of the average value of apparent power. In *2019 international conference on protection and automation of power system (IPAPS)*, (pp. 38–43). Iran: IEEE.
23. Nayak, P. K., & Pradhan, G. (2019). Detection of three-phase fault during power swing using zero frequency filtering. *International Transactions on Electrical Energy Systems*, *29*(1), e2700.
24. Biswas, S., & Nayak, P. K. (2019). An unblocking assistance to distance relays protecting TCSC compensated transmission lines during power swing. *International Transactions on Electrical Energy Systems*, e12034.
25. Alsyoufi, Y. R., & Hajjar, A. A. (2019). A high-speed algorithm to discriminate between power swing and faults in distance relays based on a fast wavelet. *Electric Power Systems Research*, *172*, 269–276. https://doi.org/10.1016/j.epsr.2019.03.021.
26. Taheri, B., Salehimehr, S., & Razavi, F. (2019). A New Method for Fast Power Swing Detection Using the Rate of Change of Energy in the Current Signal. In *27th Iranian Conference on Electrical Engineering (ICEE2019)*.
27. Taheri, B., Faghihlou, M., Salehimehr, S., & Razavi, F. (2020). A fast Fourier transform-based method for power swing detection and distance relay malfunction prevention. *Journal of Control, Automation and Electrical Systems, 31* 1–11.
28. Taheri, B., & Sedighizadeh, M. (2020). *Detection of power swing and prevention of mal-operation of distance relay using compressed sensing theory*. Transmission & Distribution: IET Generation.
29. Alizadeh, B. A. M., Khederzadeh, M., & Razzaghi, R. (2020). Fault detection during power swing in thyristor-controlled series capacitor-compensated transmission lines. *Electr Power Syst Res*, *187*, 106481. https://doi.org/10.1016/j.epsr.2020.106481.
30. Ghalesefidi, M. M., & Ghaffarzadeh, N. (2019). A new phaselet-based method for detecting the power swing in order to prevent the malfunction of distance relays in transmission lines. *Energy Systems*, 1–25.
31. Taheri, B., Hosseini, S. A., Askarian-Abyaneh, H., & Razavi, F. (2019). Power swing detection and blocking of the third zone of distance relays by the combined use of empirical-mode decomposition and Hilbert transform. *IET Generation, Transmission & Distribution*, *14*(6), 1062–1076.
32. P. Kundur, N. J. Balu, and M. G. Lauby, Power system stability and control. McGraw-hill New York, 1994.
33. Taheri, B., Faghihlou, M., Salehimehr, S., & Razavi, F. (2020). Symmetrical fault detection during power swing using mean value of sampled data from the

current signal. *IETE J Res*, 1–13. https://doi.org/10.1080/03772063.2020.1798823.
34. Nikolaev, N. Y., & Iba, H. (2003). Polynomial harmonic GMDH learning networks for time series modeling. *Neural Netw*, *16*(10), 1527–1540. https://doi.org/10.1016/S0893-6080(03)00188-6.
35. Hashemi, S., Sanaye-Pasand, M., & Shahidehpour, M. (2017). Fault detection during power swings using the properties of fundamental frequency Phasors. *IEEE Transactions on Smart Grid*.
36. Lin, X., Gao, Y., & Liu, P. (2008). A novel scheme to identify symmetrical faults occurring during power swings. *IEEE Transactions on Power Delivery*, *23*(1), 73–78. https://doi.org/10.1109/TPWRD.2007.911154.